THE ASTROPHYSICAL JOURNAL, 413:324–332, 1993 August 10

SUCCESSIVE X-RAY BURSTS FROM ACCRETING NEUTRON STARS

RONALD E. TAAM,[1,2] S. E. WOOSLEY,[2,3] T. A. WEAVER,[2] AND D. Q. LAMB[4]

Received 1992 October 14; accepted 1993 February 19

ABSTRACT

The evolution of a neutron star undergoing a series of thermonuclear flashes in its accreted hydrogen-rich layer has been numerically followed to determine the effects of the history of the neutron star's thermal and compositional structure on the properties of the emitted X-ray bursts. The burst characteristics have been studied for a range of mass accretion rates, CNO abundances in the accreted matter, and initial thermal states of the underlying neutron star core. It is found that the bursts exhibit erratic behavior, especially for low CNO metal abundances and cool neutron star cores, with the burst recurrence time scales varying by one to two orders of magnitude. The results of the calculations directly illustrate the importance of compositional and thermal inertia on burst behavior. A common characteristic of these models is the continued presence of a substantial amount of unburnt hydrogen in the accreted layer throughout the series of the X-ray burst events. Convective mixing during the quiescent phase leads to the inward transport of helium to high densities and eventually to the initiation of the next outburst. The resulting bursts can be weak and, in such cases, are characterized by short recurrence time scales ($\sim$1–2 hr), low peak luminosities ($\sim$0.1–0.2 times the Eddington value), and low α-values ($\sim$20). The numerical results indicate that such mixing can lead to an irregular pattern of unstable nuclear burning, and it is suggested that this irregularity is manifested as the erratic bursting behavior seen in X-ray transients like 1608 − 522 and EXO 0748 − 67.

Subject headings: accretion, accretion disks — stars: neutron — X-rays: bursts

1. INTRODUCTION

There is a widespread consensus that thermonuclear flashes in the surface layers of an accreting neutron star are responsible for the type I X-ray burst phenomenon (for a recent discussion of the observational and theoretical status of the X-ray burst phenomenon see the review by Lewin, van Paradijs, & Taam 1993). The model as originally proposed by Woosley & Taam (1976); see also Joss 1977; Lamb & Lamb 1978) successfully reproduces the energetics of the observed bursts ($\sim 10^{38}$–10^{39} ergs), their time scales (rise time $\sim$ several seconds; burst duration $\sim$ 10–100 s; recurrence time $\sim$ several hr), and the spectral softening seen during burst decay.

Although these general properties can be adequately described by the thermonuclear flash model, a number of outstanding problems remain when observations and theory are confronted in detail. Among these is the lack of correlation between the persistent level of emission and the burst behavior seen in some burst sources (e.g., 1735 − 44, Lewin et al. 1980; Ser X − 1, Li et al. 1977; 1608 − 522, Murakami et al. 1980; EXO 0748 − 67, Gottwald et al. 1986). For example, the recurrence time scale is observed to vary between 2 and 36 hr in 1735 − 44 and between $\sim$3 and 16 hr in EXO 0748 − 67 without a significant change in the persistent X-ray flux. Despite the irregularity in the recurrence patterns, there is evidence for a global correlation between the ratio of persistent flux to time-averaged burst flux and the burst duration with the mass accretion rate (van Paradijs, Penninx, & Lewin 1988). Erratic recurrence patterns are very difficult to comprehend if the burst properties are controlled solely by the mass accretion rate. Thus, other physical parameters which influence the structure of the neutron star envelope must be invoked.

It was first pointed out by Taam (1980) that the thermal and compositional inertia of the neutron star envelope would have important consequences on subsequent X-ray bursts. It is only by numerically calculating a succession of X-ray bursts in detail that the heating associated with the previous thermonuclear flashes and the compositional changes associated with nuclear burning in the accreted layer can be fully taken into account (e.g., Ayasli & Joss 1982; Woosley & Weaver 1985). In this manner, the relationship between the internal properties of the neutron stars and the observed characteristics of the resulting X-ray bursts can be fully evaluated. Particularly noteworthy, in this regard, are the calculations carried out by Woosley & Weaver (1985). In their study, a total of 12 X-ray bursts were followed in succession in one evolutionary sequence. The results obtained from this calculation revealed a tendency for the bursts to exhibit highly regular behavior for a neutron star, characterized by a base envelope temperature of $\sim 2 \times 10^8$ K, which accretes a nearly solar metal abundance ($Z = 0.02$) at a rate of $2 \times 10^{-9}\ M_\odot\ \mathrm{yr}^{-1}$. Some indications of erratic behavior were found for lower metallicities and lower mass accretion rates, but no definitive conclusions could be drawn due to the limited number of flashes that were followed in these cases. In addition, the sensitivity of the burst properties to the assumed initial thermal state of the neutron star core was not investigated.

In this paper we report the results of numerical calculations of the evolution of a neutron star undergoing a series of thermonuclear flashes in its accreted hydrogen-rich layer. We

[1] Department of Physics and Astronomy, Northwestern University, Evanston, IL 60208.
[2] General Studies Group, Physics Department L298, Lawrence Livermore National Laboratory, P.O. Box 808, Livermore, CA 94550.
[3] UCO/Lick Observatory, Board of Studies in Astronomy and Astrophysics, University of California, Santa Cruz, CA 95064.
[4] Department of Astronomy and Astrophysics, University of Chicago, 5640 S. Ellis Ave., Chicago, IL 60637.

examine the influence of the repeated thermonuclear flashes on the thermal state and composition of the neutron star, and the feedback which such flashes have on the subsequent X-ray burst behavior. We find that the observed erratic correlations between burst properties and the persistent emission (assumed to reflect the mass accretion rate) can be explained in terms of the evolution of the thermal and compositional structure in the neutron star envelope. These effects are particularly important for low initial neutron star core temperatures ($T \sim 10^7$ K) which lead to the accumulation of a thick, massive accreted envelope of $\sim 10^{22}$–10^{23} g. In the next section we describe the results of our calculations for a range of mass accretion rates, CNO abundances in the accreted matter, and initial thermal states of the neutron star core. The implications for the observed properties of X-ray bursts are discussed in the last section.

2. RESULTS

The structure and thermal and nuclear evolution of a neutron star envelope were calculated with the KEPLER computer program (Weaver, Zimmerman, & Woosley, 1978) modified to include the detailed input physics relevant for the study of the X-ray burst phenomenon (Wallace, Woosley, & Weaver 1982; Taam 1985; Woosley & Weaver 1985; see also Fushiki et al. 1992). The initial envelope models, which were constructed in thermal equilibrium, are characterized by their mass (ranging from 10^{-8} to 10^{-7} $M_\odot$), the luminosity of the neutron star core, $L_{\rm core}$, or equivalently the temperature at the base of the envelope, $T_{\rm env}$, the mass abundance of the accreted CNO nuclei, $Z_{\rm CNO}$, and the mass accretion rate, $\dot{M}$ (see Table 1). The mass and radius of the neutron star are chosen to be 1.4 $M_\odot$ and 9.1 km, respectively, and the hydrogen mass abundance of the accreted matter is taken to be $X = 0.7$.

2.1. *Sequence 1*

In the first sequence, which will henceforth be denoted as the standard sequence, we set the abundance of the CNO nuclei in the accreting matter equal to zero. This limiting case has some physical justification if the CNO abundance of the matter transferred from the neutron star's binary companion is significantly depleted by nuclear spallation processes in an accretion shock (see Bildsten, Salpeter, & Wasserman 1992).

For an imposed core luminosity of 3.85 $L_\odot$ the temperature and density at the base of the calculated envelope of mass 2×10^{26} g was 3.27×10^8 K and 5×10^9 g cm^{-3}, respectively. In this sequence, matter was accreted for a period of 66.25 days at which point a thermonuclear flash developed initiated by hydrogen burning accelerated by electron capture processes at high densities ($\sim 10^7$ g cm^{-3}). The nuclear burning development is similar to that described in Fushiki et al. (1992). The large amount of mass accreted ($\sim 1.4 \times 10^{23}$ g) is a result of the fact that hydrogen burning occurs only via the feeble *pp* chain in the absence of CNO nuclei. Since the rate of burning is determined by the $p(p, e^+\nu)D$ reaction, which is slow and weakly temperature sensitive, hydrogen burning in this case can only initiate instability at densities sufficient that electron capture processes significantly enhance the energy generation rate. In contrast to the work of Fushiki et al. (1992), where emphasis was placed on obtaining an understanding of the long X-ray tail behavior of the first burst emitted by the neutron star during a soft X-ray transient event, we concentrate on the long-term behavior of bursts after a number of bursts have been calculated.

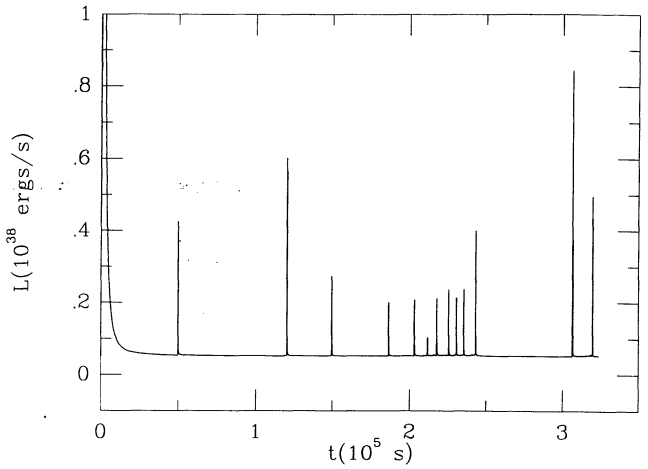

FIG. 1.—Temporal luminosity variations from the neutron star surface in the standard sequence for which the accreted matter consists of hydrogen and helium only. Note that the recurrence patterns are very irregular ranging from 1.3 to 17.6 hr after the first three burst events. Of particular interest is the increase of the waiting time from the preceding burst from 2.15 to 17.6 hr for bursts 12 and 13. The luminosity, which includes the contribution from accretion, is in units of 10^{38} ergs s^{-1}, and the unit of time is 10^5 s. The origin of time has been shifted to the occurrence of the first burst for clarity.

The resulting light curve for 14 bursts is displayed in Figure 1. The first burst nearly reaches the Eddington limit at 1.97×10^{38} ergs s^{-1} at peak light and lasts for an *e*-folding decay time scale of ~ 3000 s. This burst is the most energetic of the sequence and is characterized by an energy of $\sim 5 \times 10^{41}$ ergs. The energy for the outburst is primarily derived from the helium burning reactions during the early phase and by the hydrogen burning reactions during the long X-ray tail (see Fushiki et al. 1992). Because the ignition occurs at high pressures ($\sim 3 \times 10^{24}$ dyne cm^{-2}) the electron degeneracy of the accreted layer was not lifted until the temperatures had peaked at 3×10^9 K.

The next five bursts have peak luminosities less than 6×10^{37} ergs s^{-1} and waiting times of 13.8, 19.6, 8.1, 10.2, and 4.6 hr, respectively. The energies of these bursts are roughly

TABLE 1

PARAMETERS OF X-RAY BURST SEQUENCES

Sequence	$L_{\rm core}(L_\odot)$	$T_{\rm env}(10^8$ K)	$Z_{\rm CNO}$	$\dot{M}$ ($M_\odot$ yr^{-1})	Burst Behavior
1.....	3.85	3.27	0	4×10^{-10}	Highly erratic
2.....	1.92	2.37	0.001	4×10^{-10}	Erratic
3.....	0.13	0.584	0.001	4×10^{-10}	Highly erratic
4.....	0.13	0.648	0.02	4×10^{-10}	Trend to regular
5.....	0.13	0.648	0.02	1×10^{-10}	Regular

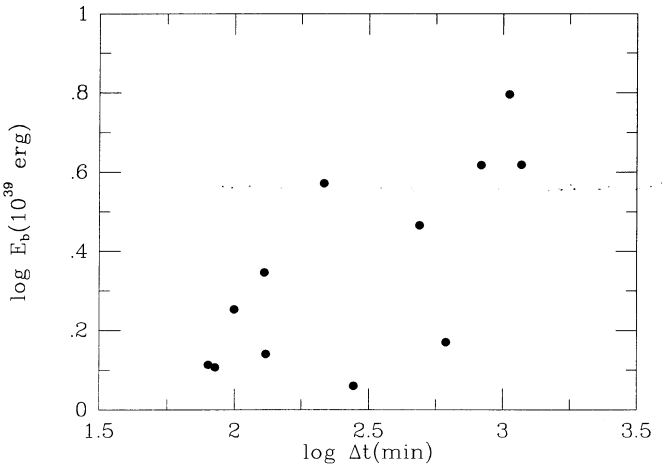

FIG. 2.—Distribution of the energy emitted in the outburst with respect to the recurrence time from the preceding burst for all bursts except the first burst in the standard sequence. Note that there is a tendency for a clustering of weak bursts for recurrence time scales in the vicinity of 100 minutes. The units of energy and recurrence time are 10^{39} ergs and minutes, respectively.

correlated with the recurrence time to a preceding burst and vary by a factor of 3.5 from 1.2×10^{39} ergs to 4.2×10^{39} ergs (see Fig. 2). Note that after the emission of the sixth X-ray burst (see Fig. 1), about 56 hr after the emission of the first burst, the burst behavior becomes nearly regular with the recurrence time of the next six bursts clustering together (see Fig. 2) and ranging between 1.3 and 2.4 hr. These dwarf-like bursts have peak burst luminosities $\lesssim 4 \times 10^{37}$ ergs s^{-1} and emit $\lesssim 3 \times 10^{39}$ ergs in the outburst. The light curve of the individual bursts vary little from burst to burst and are similar to that of the twelfth burst in the sequence shown in Figure 3. The rise time and *e*-folding decay time scale of the burst are ~ 20 and ~ 50 s, respectively. The time averaged burst emission is $\sim 3 \times 10^{35}$ ergs s^{-1} which yields a ratio for the accretion luminosity to the time-averaged burst luminosity (known as α) ~ 18. This α-value is anomalously low in view of the fact that hydrogen has been depleted by only $\sim 20\%$ in the burning layers. This implies that the energy for the outburst is produced not only by the matter accreted between bursts, but also by matter which had not yet been synthesized to iron peak elements in previous outbursts (see below).

The thermonuclear burning during these weak bursts is not effective in heating the neutron star interior since the flash develops in the outer surface layers ($\lesssim 3 \times 10^{20}$ g) where the thermal structure of the envelope is effectively decoupled from that of the interior (Fujimoto et al. 1984, 1987a). As a result, the interior cools during the quiescent phases between the weak bursts, and the internal temperature in the accreted layer decreases from $\sim 4 \times 10^8$ to 3×10^8 K. The sequence of weak bursts ends when the temperature becomes so low that the mixing which eventually follows each burst (see below) is insufficient to initiate another burst.

Consequently, the waiting time to the next burst in the sequence (i.e., after the semiregular sequence of seven bursts; see Fig. 1) increased to 17.6 hr (about 8 times longer than the waiting time of the preceding outburst). The energy of the outburst also increased, but only by a factor of 2.8 to 6.3×10^{39} ergs, increasing α to 52. Since the amount of accreted matter is much larger ($\sim 1.6 \times 10^{21}$ g), heating of the interior region is more effective, and the waiting time to the fourteenth burst is reduced to 3.6 hr. The effectiveness of this heating is clearly illustrated by the evolution of the temperature distribution (see Fig. 4) which shows that a substantial part of the accreted layer interior to the main burning shell has been heated by the outburst. During the burst inactive phases, the cooling of the neutron star envelope contributes to the quiescent luminosity at a level of $\gtrsim 10^{35}$ ergs s^{-1}, with a greater amount produced by nuclear burning for those phases where the waiting times are shorter.

Table 2 lists the recurrence time from the preceding burst, the peak burst luminosity, the burst energy, and the resulting α-value for each of the bursts in sequence 1. The distribution of burst peak luminosities with respect to the recurrence time from the preceding burst is illustrated in Figure 5 for all bursts except the first. The moderate correlation between these two properties is comparable to that between the burst energy and recurrence time scale (see Fig. 2). The distribution of burst

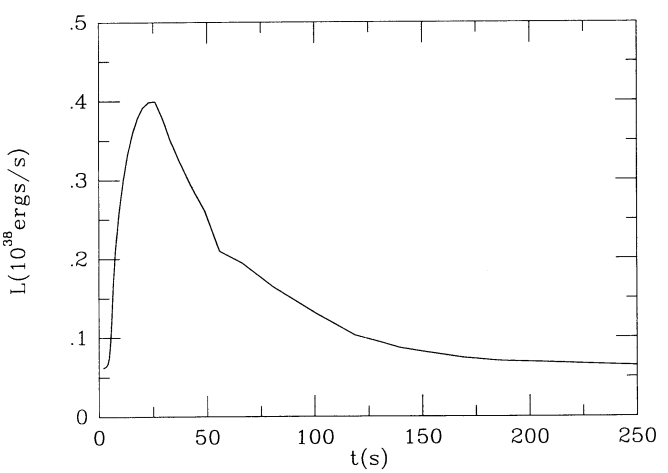

FIG. 3.—Light curve for the twelfth burst in the standard sequence. The energy of the outburst is 2.2×10^{39} ergs and the ratio of the accretion luminosity to the time-averaged burst emission is 18.

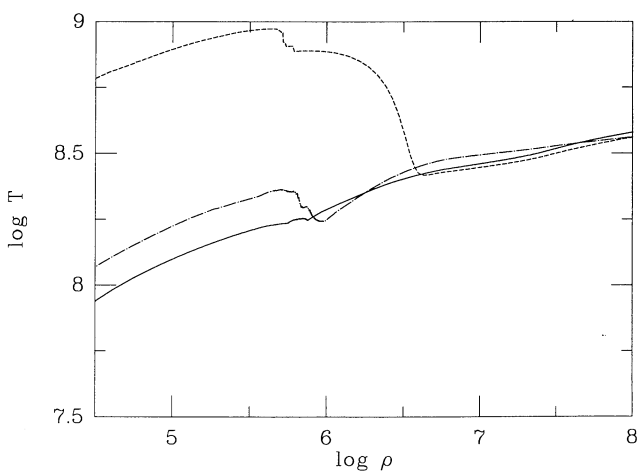

FIG. 4.—Temperature distribution in the neutron star envelope before, during and after the occurrence of the penultimate burst in the standard sequence 1. Note that about 8.1 hr before the burst (*solid curve*) the temperature profile is relatively flat at depth reaching a maximum of $\sim 4 \times 10^8$ K. At the peak of the outburst (*dashed curve*) the temperature in the outermost 1500 cm of the neutron star is elevated to a maximum of $\sim 10^9$ K. About 1.6 hr after the outburst (*dash-dotted curve*) the temperature distribution has become flatter at depth for $\rho \gtrsim 10^7$ g cm^{-3}.

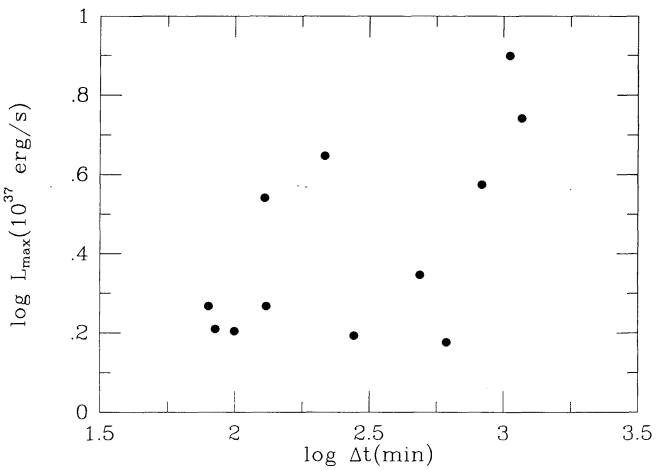

FIG. 5.—Distribution of the peak burst luminosity with respect to the recurrence time from the preceding burst in the standard sequence. The luminosity is in units of 10^{37} ergs s^{-1}, and the recurrence time is in minutes.

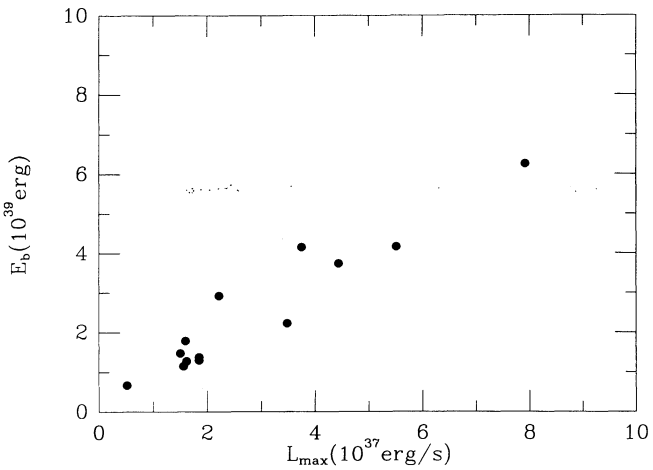

FIG. 6.—Distribution of the peak burst luminosities (in units of 10^{37} ergs s^{-1}) with respect to the energy emitted in the burst (in units of 10^{39} ergs). A positive correlation between these two observables is evident with the more energetic bursts characterized by higher peak luminosities.

energies with respect to the peak luminosity (see Fig. 6) shows a stronger correlation. In addition, we point out the existence in Figure 6 of a cluster of weak bursts having luminosities that are a factor of 10 below the Eddington luminosity. These weak bursts can be understood in terms of the detailed compositional evolution discussed below.

The nuclear burning that occurs during the evolution of the X-ray burst is quite complicated. Among other aspects, it leads to the creation of ^{14}N (the most abundant of the CNO group), even though the accreted matter contains no ^{14}N. The ^{14}N is created in a spatially limited region (see Fig. 7) whereas hydrogen (with a hydrogen mass abundance of 0.55), as well as Ni and Fe, are present throughout nearly the entire accreted layer. Thus substantial amounts of hydrogen have survived the preceding thermonuclear flashes. We point out that the hydrogen abundance increases while the Ni abundance decreases as the presssure increases from log $P = 22.1$ to log $P = 23.7$. This unusual situation is a consequence of the operation of β decay and proton capture reactions on intermediate mass nuclei via the *rp* process at a late burning stage of the thermonuclear outburst. As a result of this spatial variation in composition, the mean molecular weight increases outwards in this region. The region is therefore Rayleigh-Taylor unstable (an instability which is also known as the classical salt finger instability). In the present circumstance it is initially stabilized by an inverted temperature gradient (see Fig. 8 and Woosley & Weaver 1985) due to the spatial variation of the energy generation rate associated with (α, γ) reactions on intermediate mass nuclei. However, the stability is only temporary. When the inverted temperature gradient disappears as a result of radiative cooling from the neutron star surface, the region becomes unstable. Mixing of matter then occurs. In particular, following the eleventh X-ray burst, helium is mixed to a depth of $\sim 2 \times 10^{21}$ g (about a factor of 10 larger in mass than that accreted between outbursts). As a result the newly mixed helium burns to ^{12}C which, itself, rapidly captures protons to produce ^{14}N. In so doing the ^{14}N abundance increases from 0.001 to a maximum of $\sim$0.007. These charged particle reactions initiate the next thermonuclear flash. However, the resulting X-ray burst is weak due to the low mass abundance of helium ($\sim$0.05) in the mixed layer.

TABLE 2

PROPERTIES OF X-RAY BURSTS IN SEQUENCE 1

Burst	Δt (minutes)	L_b (10^{37} ergs s^{-1})	E_b (10^{39} ergs)	α
1.....	...	19.71	545.9	...
2.....	830.4	3.75	4.15	62
3.....	1173.6	5.51	4.16	87
4.....	487.8	2.22	2.92	52
5.....	613.8	1.50	1.48	128
6.....	277.8	1.56	1.15	73
7.....	142.8	0.52	0.67	68
8.....	99.6	1.60	1.79	17
9.....	130.8	1.85	1.38	29
10.....	84.6	1.62	1.28	20
11.....	79.8	1.85	1.30	19
12.....	129.0	3.48	2.22	18
13.....	1056.6	7.92	6.25	52
14.....	215.8	4.44	3.73	18

2.2. *Sequence 2*

To investigate the dependence of the erratic behavior found in the standard sequence on the abundance of CNO in the

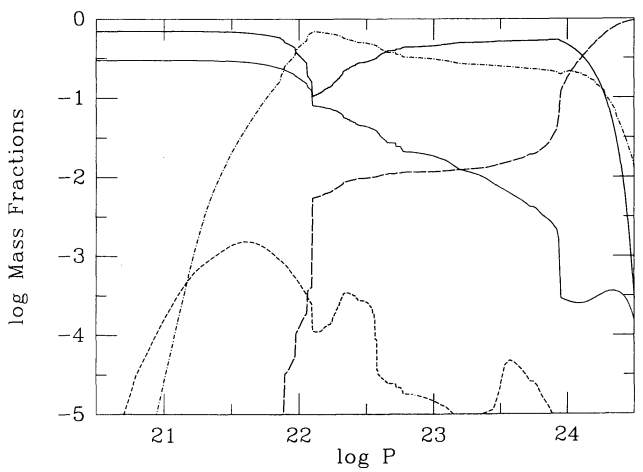

FIG. 7.—Compositional profiles as a function of the pressure at 3.17×10^5 s after the first burst (i.e., after $\sim$2.9 hr after the penultimate burst) in the standard sequence. The profiles for H, He, ^{14}N, ^{54}Fe, and ^{56}Ni are denoted by solid, dotted, short dashed, long dashed, and dash-dot curves. Note that the nickel abundance increases outwards and the hydrogen abundance decreases outwards in a restricted range of the envelope. Note further the existence of substantial hydrogen throughout the accreted envelope.

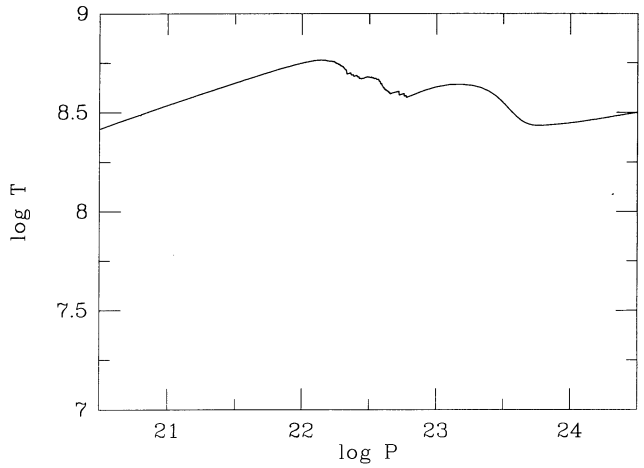

FIG. 8.—Temperature distribution at the same point in time as Fig. 7. Note the presence of a temperature inversion in the region where the hydrogen abundance decreases outwards. It can be seen that there are three temperature inversions which mark the cumulative effects of the heating associated with the previous outbursts.

accreted matter, we increased Z_{CNO} to 0.001 in sequence 2. The temperature at the bottom of the envelope was decreased slightly to 2.37×10^8 K. For this sequence 12 bursts were followed (see Fig. 9). It can be seen that two types of bursts are emitted, one characterized by peak luminosities comparable to the Eddington limit and the other a factor of 4–5 weaker. The relative peaks and waiting times between these bursts are reminiscent of the type observed for bursts with short (5–10 minute) intervals (see Lewin et al. 1976; Oda 1982; Gottwald et al. 1986); however, the actual waiting times are much too long in this sequence. In particular, the waiting times appear very regular for the luminous bursts with time scales ranging from 26 to 34 hr. For some bursts the peak luminosities exceeded the Eddington limit, and a finer zoned calculation would have led to a phase of mass loss. Except for the second and third outbursts, a weaker burst ($L_{max} \lesssim 6.5 \times 10^{37}$ ergs s^{-1}) is emitted within a time ranging from $\sim$2.8 to 4.4 hr (see Fig. 9). Table 3 lists the recurrence time from the preceding burst, the peak burst luminosity, the burst energy, and the resulting α-value for each of the bursts in sequence 2.

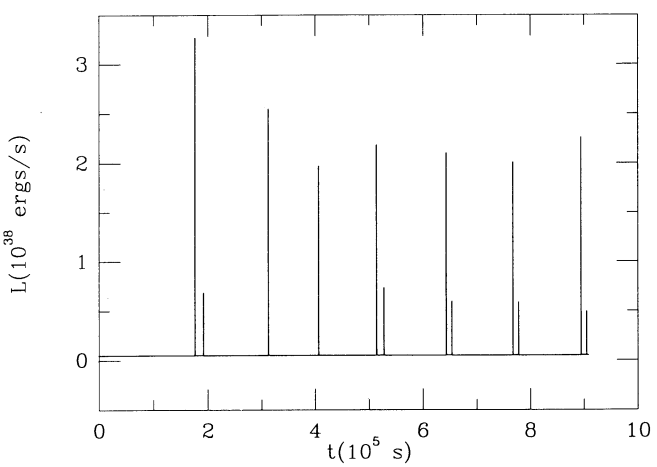

FIG. 9.—Light curve for sequence 2. The origin of time corresponds the onset of accretion. The units are the same as in Fig. 1. Note that the outbursts are punctuated with phases where a single dwarf burst follows a normal burst.

TABLE 3

PROPERTIES OF X-RAY BURSTS IN SEQUENCE 2

Burst	Δt (minutes)	L_b (10^{37} ergs s^{-1})	E_b (10^{39} ergs)	α
1.....	...	32.19	16.90	...
2.....	262.2	6.37	3.34	24
3.....	2010.0	24.96	11.00	57
4.....	1561.8	19.18	9.10	53
5.....	1789.8	21.33	9.89	56
6.....	232.2	6.60	3.35	22
7.....	1923.6	20.51	10.00	60
8.....	171.6	5.45	3.31	16
9.....	1900.8	19.57	9.53	62
10.....	177.0	5.36	3.29	17
11.....	1942.8	22.08	10.20	59
12.....	169.2	2.99	4.44	18

If we group the main burst and its subsequent weaker burst together, it appears that the burst pattern is fairly regular. This type of burst behavior is distinct from that seen in the previous sequence and illustrates the diversity that can result from the convective mixing mechanism.

2.3. *Sequence 3*

To determine the generality of the erratic behavior found in the standard sequence, we held Z_{CNO} at the value of 0.001 assumed in sequence 2 and decreased the core luminosity to 0.13 $L_\odot$. The resulting temperature and density at the base of the calculated envelope of mass 1.6×10^{26} g were 5.84×10^7 K and 4.24×10^9 g cm^{-3}, respectively. In this case 9.6×10^{22} g was accreted before the onset of the thermonuclear flash. Even though Z_{CNO} was larger than in sequence 1, the amount of mass accreted before the initial outburst did not differ significantly. This is due to the low temperatures ($T \sim 10^7$ K) in the hydrogen-rich accreted layers. The nuclear burning development was nearly identical to the standard sequence, but the heating of the neutron star core was far more dramatic due to the lower initial temperatures assumed. In particular, the temperatures in the iron substrate near the base of the accreted layer increased from $\sim 2 \times 10^7$ K before the first outburst to $\sim$2–3 $\times 10^8$ K after all subsequent outbursts. This is to be compared to temperatures of $\sim 2 \times 10^8$ K before the outburst and $\sim 4 \times 10^8$ K after the outbursts in the standard sequence. Although the temperatures produced in the interior differed in the two sequences, the thermonuclear runaways resulted in similar X-ray bursts characteristics. In particular, 12 bursts were followed, and the light curve for the entire evolution is illustrated in Figure 10.

After the first four bursts a nearly regular recurrence pattern behavior was reached. The next five bursts were dwarf-like ($L_{max} \lesssim 2 \times 10^{37}$ ergs s^{-1}) and were characterized by an average recurrence time between bursts of $\sim$1.6 hr. The energies of these bursts were $\sim$1–2 $\times 10^{39}$ ergs, and their corresponding α-values ranged from 15 to 23. This regularity, however, was interrupted by the tenth burst in the sequence, which occurred after a waiting time of 11.05 hr (in contrast to the preceding burst which had a waiting time of 1.7 hr) due to the inability of the sequence of weak bursts to maintain the envelope at elevated temperatures. As a result, α increased by nearly a factor of 3 from 15 to 42. As in the standard sequence the deep envelope heating resulting from this thermonuclear flash led to a reduction in the recurrence times to the next two bursts (3.46 and 2.76 hr). Hence, the strongly erratic behavior found in the standard sequence extends to cases where the abundance of the accreted CNO elements is non-zero if the

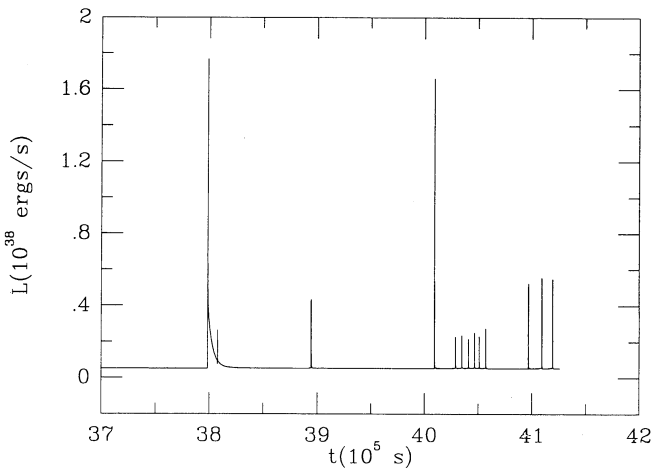

FIG. 10.—Light curve for sequence 3. The units are the same as in Fig. 1. The origin of time corresponds to the onset of accretion onto the neutron star. Note the irregular behavior of the waiting time from the preceding bursts in the last 5 bursts in the sequence.

temperature of the neutron star core is low enough. The distribution of peak luminosities and burst energies with recurrence times is also similar to that found for the standard sequence; however, a stronger correlation exists between the burst energy and the recurrence time (see Fig. 11) in the sense that the more energetic bursts have longer waiting time scales. Although the correlation is not strictly followed for all bursts, it seems to hold on average.

Table 4 lists the recurrence time from the preceding burst, the peak burst luminosity, the burst energy, and the resulting α-value for each of the bursts in sequence 3. These results and those for sequence 2 suggest that the convective mixing mechanism is less effective in producing a series of low luminosity bursts at higher internal temperatures. This is consistent with the results of Woosley & Weaver (1985) who did not find a series of dwarf bursts of the type found in sequences 1 and 3 for their models characterized by high core internal temperatures. If we group the main burst and its subsequent weaker burst together (in sequence 2), it appears that the burst pattern becomes more regular as the internal temperature of the neutron star core is increased for models with non-zero CNO abundances. This behavior is related to the fact that hydrogen

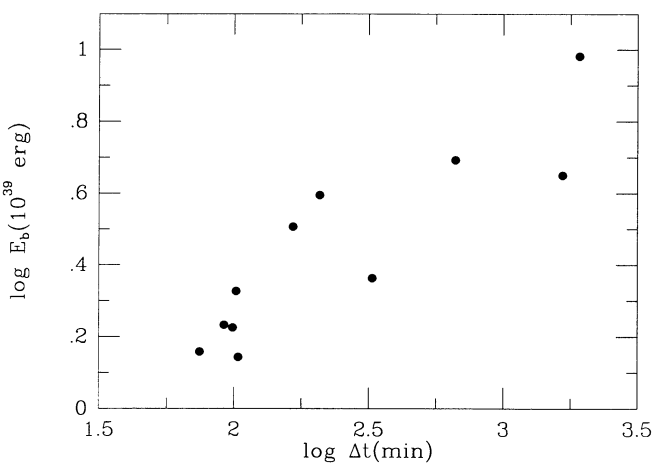

FIG. 11.—Distribution of burst energies (in units of 10^{39} ergs) with respect to the recurrence time (in minutes) to the previous burst in sequence 3. The more energetic bursts usually require a longer waiting time to outburst.

TABLE 4

PROPERTIES OF X-RAY BURSTS IN SEQUENCE 3

Burst	Δt (minutes)	L_b (10^{37} ergs s^{-1})	E_b (10^{39} ergs)	α
1.....	...	6.38	164.0	...
2.....	1660.2	3.82	4.47	115
3.....	1915.8	15.69	9.59	62
4.....	325.3	1.76	2.31	44
5.....	99.0	1.83	1.68	18
6.....	103.8	1.65	1.39	23
7.....	91.8	1.99	1.71	17
8.....	74.4	1.79	1.44	16
9.....	102.0	2.26	2.12	15
10.....	663.0	4.73	4.93	42
11.....	207.6	5.05	3.93	16
12.....	165.6	4.98	3.21	16

is nearly depleted at depth in sequence 2, in contrast to sequences 1 and 3. In particular, the hydrogen mass abundance throughout the envelope (excluding the freshly accreted hydrogen) is $\lesssim 0.1$ in sequence 2.

2.4. *Sequence 4*

The results of Woosley & Weaver (1985) indicated that the behavior of the waiting times between bursts becomes more regular with increasing CNO abundances. To determine whether this trend is dependent on the internal thermal state of the neutron star we considered sequence 4 in which the temperature at the inner boundary was chosen to be 6.48×10^7 K and the mass abundance of the CNO nuclei was increased to 0.02. Because the temperatures are about a factor of 3 lower than that adopted by Woosley & Weaver (1985) the first burst occurred after $\sim 3.8 \times 10^{22}$ g of matter was accreted. This is 2.5 times less than that accreted in sequence 3 and more than 20 times the mass accreted in model 2 of Woosley & Weaver (1985). These comparisons illustrate that the critical accumulated mass required to initiate the instability is more sensitive to the thermal state of the neutron star than to the CNO abundance of the accreted matter.

The light curve for the 14 bursts in the sequence is illustrated in Figure 12. It is evident that there is a tendency for the recurrence time scale to decrease from burst to burst. This progression to shorter waiting times continued until a nearly

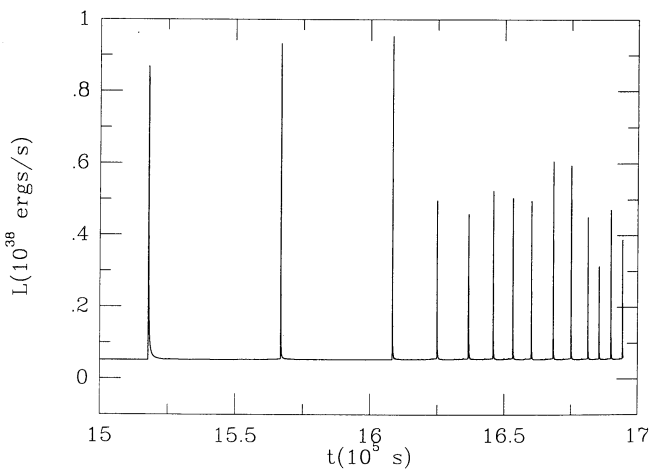

FIG. 12.—Light curve of the bursts for sequence 4. The luminosity is in units of 10^{38} ergs s^{-1}, and the unit of time is 10^5 s. The weaker bursts exhibit a very nearly regular behavior with the burst recurrence time scales varying slightly. The peak luminosities are comparable to the last burst of sequence 3 and are about a factor of 2 more luminous than its associated dwarf-life bursts.

regular behavior was established 18.75 days after the onset of accretion. At this time the temperatures near the base of the entire accreted layer in the Fe substrate were typically 2×10^8 K (comparable to the initial temperatures at the base of the envelopes assumed by Woosley & Weaver 1985). As a consequence of these elevated envelope temperatures the recurrence times for burst number 5–14 decreased from the earlier evolutionary phase and ranged between 1.2 and 3.3 hr. The bursts occurred more frequently, at times, than found for model sequence 2 of Woosley & Weaver (1985), where the recurrence time scale was 2.4 hr, even though the accretion rate is lower by a factor of 5 in the present case. Furthermore, these bursts are less luminous by a factor of 2–3 than found by Woosley & Weaver (1985) which suggests that the existence of dwarf-like bursts is dependent on the mass accretion rate. In contrast to the previous sequences described above, there is no evidence of erratic behavior in the burst waiting times.

Table 5 lists the recurrence time from the preceding burst, the peak burst luminosity, the burst energy, and the resulting α-value for each of the bursts in sequence 4. The distribution of burst energies and peak luminosities are plotted versus recurrence time scale in Figures 13 and 14, respectively. The burst energies range from 1.9 to 7.8 $\times 10^{39}$ ergs, and the peak luminosities range from 2.6 to 9 $\times 10^{37}$ ergs s^{-1}. In contrast to the previous sequences the correlations between the burst energy and peak luminosity with recurrence time are stronger with a tighter relation existing for the relation between the burst energy and waiting time scale. As in previous sequences, there is also a tendency for a clustering of bursts near $\Delta t \sim 100$ minutes. However, in this sequence the peak burst luminosities for the dwarf-like bursts are higher by a factor of about 2 than found in the cases of low CNO abundances.

2.5. *Sequence 5*

In all the previous sequences the mass accretion rate onto the neutron star was fixed at $4 \times 10^{-10}\ M_\odot\ \mathrm{yr}^{-1}$. To investigate the sensitivity of our results to variations in the accretion rate we decreased the rate to $10^{-10}\ M_\odot\ \mathrm{yr}^{-1}$ in sequence 5, but all other parameters were chosen to be the same as in sequence 4. Table 6 lists the recurrence time from the preceding burst, the peak burst luminosity, the burst energy, and the resulting α-value for each of the bursts in sequence 5. The numerical results reveal that the burst behavior is much less erratic than in the first three sequences, and it appears to reach a regular state after the initial transient phase. In particular, after the first four bursts, the recurrence time scales ranged from ~ 31 to 34 hr. This is more than a factor of 10 longer than the recurrence time scales found for the long-term behavior of bursts in sequence 4 (and, in fact, is comparable to that found in sequence 2) and is greater than that expected from the change in the mass accretion rate. This nonlinear scaling reflects the fact that the temperature has also decreased which, therefore, requires a greater accumulated mass to initiate the thermonuclear instability. Specifically the temperatures in the Fe substrate are $\lesssim 1.5 \times 10^8$ K, which are lower than found in sequence 4 since there is more time available during the quiescent phase for the envelope to cool. The last four bursts are characterized by peak luminosities of 1–1.5 $\times 10^{38}$ ergs s^{-1} (see Fig. 15) and energies ranging from 5.4–8.2 $\times 10^{39}$ ergs (corresponding to α-values of 20–30).

Unlike the previous sequences there is no evidence for the production of dwarf-like bursts. On the other hand, in this sequence, as in the other sequences, the energy released in the outburst is produced, in part, in mass layers which had been accumulated previous to the preceding outburst. We note that due to the large mass ($\sim 4 \times 10^{22}$ g) of hydrogen in the envelope which was required to initiate the first outburst, the nuclear burning behavior is of the combined hydrogen-helium

TABLE 5

PROPERTIES OF X-RAY BURSTS IN SEQUENCE 4

Burst	Δt (minutes)	L_b (10^{37} ergs s^{-1})	E_b (10^{39} ergs)	α
1.....	...	8.17	15.26	...
2.....	814.2	8.80	5.46	46
3.....	691.8	9.02	7.77	28
4.....	276.6	4.46	5.01	21
5.....	196.2	4.08	4.40	14
6.....	154.2	4.72	3.98	12
7.....	122.4	4.53	3.57	11
8.....	114.6	4.45	3.70	10
9.....	136.2	5.55	3.93	11
10.....	111.6	5.44	3.60	10
11.....	103.8	4.00	3.05	11
12.....	70.8	2.63	1.92	12
13.....	74.4	4.20	2.94	8
14.....	72.6	3.37	2.38	10

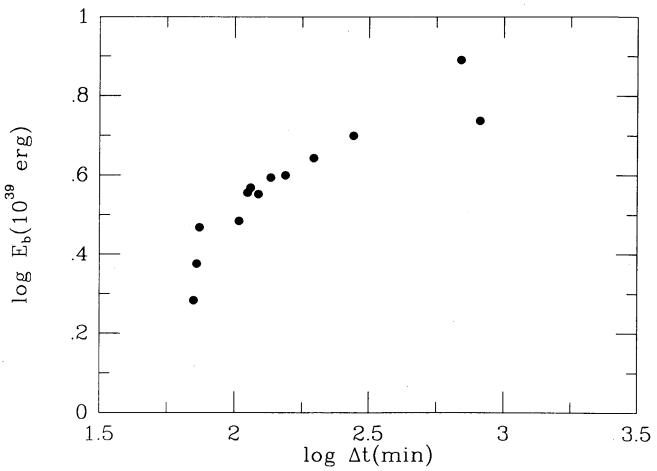

FIG. 13.—Distribution of burst energies (in units of 10^{39} ergs) with recurrence time (in minutes) from the preceding burst for sequence 4. At intermediate energies between 2.5 to 5 $\times 10^{39}$ ergs a strong correlation is evident.

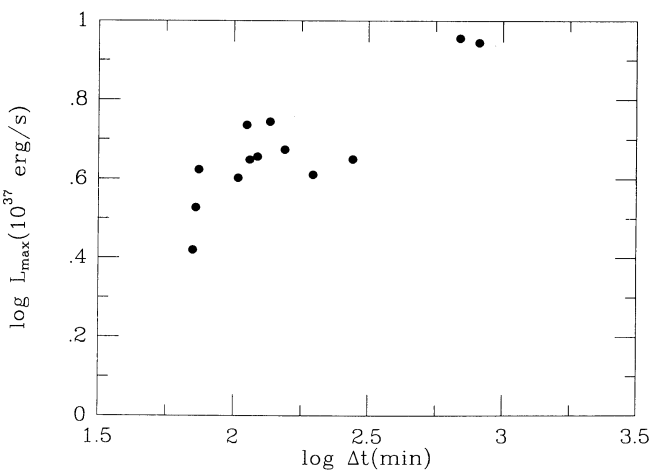

FIG. 14.—Distribution of peak luminosity (in units of 10^{37} ergs s^{-1}) with recurrence time (in minutes) from the preceding burst for sequence 4. Higher peak luminosities are generally correlated with recurrence times, but deviations occur in the relation for individual bursts.

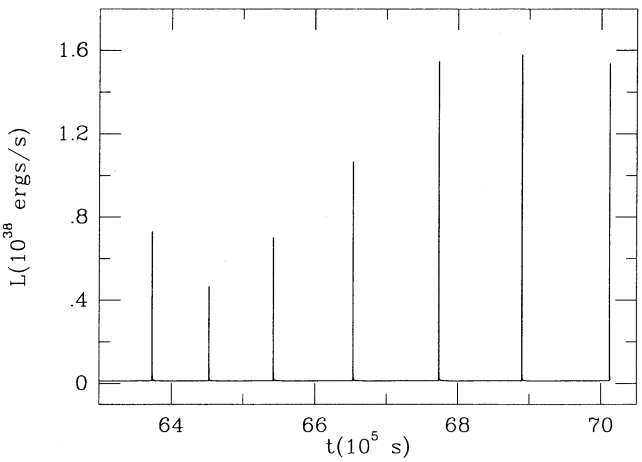

FIG. 15.—Light curve for sequence 5. The units are the same as in Fig. 1. The bursts recur at regular although not periodic intervals with no evidence for the occurrence of dwarf-like bursts.

type (with average α-values ~ 11 for the regular part of sequence 4 and ~ 23 for sequence 5) even though the temperatures in the envelope and the mass accretion rate would indicate a stable hydrogen burning shell overlying a nearly pure helium layer in a steady state description. The evolution to the steady state would require the exhaustion of the hydrogen at depth after a number of thermonuclear flashes have taken place.

3. DISCUSSION

We have demonstrated that including the thermal and compositional history of an accreting neutron star in the thermonuclear flash model of X-ray bursts can have profound consequences. The results of detailed numerical calculations of a series of thermonuclear flashes show that the time between bursts can vary by nearly an order of magnitude without any change in the mass accretion rate. These results suggest that the erratic burst behavior seen in the X-ray transients 1608−522 (Murakami et al. 1980) and EXO 0748−67 (Gottwald et al. 1986) may be explicable in terms of a cool neutron star which has accreted a thick hydrogen-rich envelope.

The occurrence of weak bursts characterized by peak burst luminosities ~ 0.1–0.2 times the Eddington value is also a common feature in the burst sequences (as are the weak bursts observed from EXO 0748−67; Gottwald et al. 1986). These weak bursts recur frequently (recurrence time scales $\lesssim 2$ hr) and have α-values ~ 20. These characteristics results from the incomplete burning of nuclear fuel in the previous outbursts coupled with the inward mixing of the accreted helium to higher density (e.g., Woosley & Weaver 1985; Fujimoto et al. 1987b) and are not predicted by the simple thermonuclear flash model. We find that unburnt nuclear fuel is commonly present in our models, and we identify a Rayleigh-Taylor instability resulting from an inversion in the mean molecular weight of the matter as the mixing mechanism. Thus the energetics of the outbursts from such sources as EXO 0748−67 (Gottwald et al. 1986) and MXB 1636−536 (Fujimoto et al. 1987b) can be reconciled with the small amount of mass accreted between the outbursts in terms of the potential nuclear energy stored in the unburnt matter from previous outbursts.

TABLE 6

PROPERTIES OF X-RAY BURSTS IN SEQUENCE 5

Burst	Δt (hr)	L_b (10^{37} ergs s^{-1})	E_b (10^{39} ergs)	α
1.....	...	8.11	15.53	...
2.....	27.5	7.18	4.89	26
3.....	21.9	4.52	3.79	27
4.....	25.0	6.89	4.01	29
5.....	30.8	10.53	5.41	26
6.....	33.3	15.34	7.15	22
7.....	32.4	15.65	6.52	23
8.....	34.0	15.24	8.18	19

The results of our calculation demonstrate that there are conditions where dwarf bursts are seen irregularly (sequences 1, 2, and 3), where dwarf bursts are seen regularly (sequence 4), and where dwarf bursts are absent (sequence 5). Erratic behavior and the dwarf-burst phenomenon are related, since erratic behavior is always accompanied by the production of dwarf bursts. The converse is not true, however, since dwarf bursts can occur without erratic behavior provided that appropriate conditions are satisfied (see sequence 4).

Further studies are needed in order to delineate quantitatively the range of mass accretion rates $\dot{M}$, CNO abundances $Z_{\rm CNO}$ in the accreted matter, and temperatures $T_{\rm env}$ in the neutron star envelope for which erratic and dwarf-like burst behavior occur. However, the results of this study indicate that both behaviors become more pronounced as $Z_{\rm CNO}$ and $T_{\rm env}$ decrease. For example, the results found for sequence 2 suggest that at $T_{\rm env} \approx 2 \times 10^8$ K the transition between erratic and regular burst behavior occurs at $Z_{\rm CNO} \approx 10^{-3}$, while the results for sequences 3 and 4 indicate that at $T_{\rm env} \approx 6 \times 10^7$ K, the transition occurs between $Z_{\rm CNO} \approx 10^{-3}$ and 0.02. Furthermore, the results for sequence 5 suggest that dwarf-like bursts occur only at mass accretion rates $\dot{M}$ above some critical value. Below this threshold, cooling of the neutron star interior between bursts is sufficient to preclude the production of such bursts.

Bildsten et al. (1992) have shown that the CNO abundances in the accreted matter can be significantly depleted by nuclear spallation processes in an accretion shock. The results of the present study indicate that regular burst behavior is not expected if the CNO abundance in the accreted matter has been significantly depleted. Sequence 1 shows that, apart from the first thermonuclear instability, the CNO abundances produced in the thermonuclear flashes themselves will determine the X-ray burst behavior if $Z_{\rm CNO} \lesssim 10^{-3}$ in the accreted matter.

The metallicities of globular cluster stars span a range $10^{-4} \lesssim Z_{\rm CNO} \lesssim 0.02$ (Smith 1987, 1988; Suntzeff 1988), as do disk and halo stars (Lambert 1987; Wheeler, Sneden, & Truran 1989). The results of the present study suggest that erratic X-ray burst behavior requires low CNO abundances in the accreted matter. Low-metallicity systems are therefore expected to exhibit erratic burst behavior while high-metallicity systems are expected to exhibit more regular burst behavior. The regularity or irregularity of X-ray burst behavior might eventually be able to be used to determine the metallicity of globular clusters in the Milky Way and in other nearby galaxies.

Erratic behavior is even more likely in X-ray transients because not only can $Z_{\rm CNO}$ be low, but $T_{\rm env}$ is also expected to be low at the onset of accretion. In particular, the results of our numerical calculations can be applied to the X-ray transient EXO 0748−67 (Gottwald et al. 1986). We find from sequences 1 and 3 that the waiting time to the next outburst can increase

by more than a factor of 6 without a change in the mass accretion rate. This is comparable to the irregular behavior seen in EXO 0748−67 when the recurrence time increased from 2.9 to 16 hr for a 50% increase in the persistent emission. Furthermore the ratio of the observed α-values for these two bursts is about 4.5, which is comparable to the value of about 3 for the ratio of the largest α-value to the smallest α-value at a given mass accretion rate for bursts exhibiting erratic behavior. If we take into account the increase in the level of persistent emission and assume that the energy of the outburst would not change instantaneously as a result of the change in the accretion rate, then a ratio of 4.5 can be obtained from the model sequences. Although the ratios of α-values can be brought into agreement, the observed α-values are larger than those produced in the model calculations by a factor of roughly 4. This difference may be attributable to anisotropy of the X-ray flux due to scattering of the X rays off the accretion disk surrounding the neutron star (see Lapidus & Sunyaev 1985; Fujimoto 1988; Melia, Zylstra, & Fryxell 1992). Because of uncertainties in the anisotropy of the X-ray flux, we do not consider the difference between the numerical calculations and the observations to be severe.

On account of the cool neutron star cores assumed in this study, the thermal structure of the neutron star envelopes during the quiescent state differs from those based upon a steady state approximation where the core luminosity is equal to the steady state nuclear luminosity (Fujimoto, Hanawa, & Miyaji 1981). Even when the envelope temperatures are high ($T > 10^8$ K) a pure helium layer does not form, because any inverted mean molecular weight gradient is eventually removed as the envelope cools, resulting in the mixing of helium with the underlying hydrogen-rich layer. The onset of the thermonuclear instability therefore occurs in a hydrogen-rich environment. Thus the X-ray burst behavior produced by an unstable helium layer underlying a stable hydrogen burning shell is not found in the models calculated here. We conjecture that such a configuration may be achieved when the underlying hydrogen accreted before the onset of the first thermonuclear instability is finally exhausted by the *pp* chain (after weeks or months), if the mass accretion rate and the CNO abundances are high enough.

Since the conditions required for the initiation of the thermonuclear instability depend upon the detailed history of the neutron star, the instantaneous value of the mass accretion rate is not necessarily strongly correlated with the properties of the X-ray bursts. For example, outbursts can occur more frequently even though the accretion rate is lower (compare sequence 4 with sequence 2 of Woosley & Weaver 1985) rather than at higher rates as expected from the simple thermonuclear flash model. A strong correlation is particularly expected to be lacking in X-ray transients like EXO 0748−67 (Gottwald et al. 1986), since the persistent emission in these sources changes on time scales of days (which is much shorter than the thermal time scale of the neutron star interior). Direct correlations as inferred from the simple model could be expected, however, if the accretion rate were constant over a thermal time scale of the neutron star.

General relativistic effects, which have been neglected in the present investigation, will modify the burst properties quoted above (see Ayasli & Joss 1982). Because the gravitational redshift factor for the assumed mass and radius of the neutron star is 1.36, the recurrence time scales should be increased by a factor of 1.36, the energies reduced by a factor of 1.36, and the luminosities reduced by a factor of 1.85. Although general relativistic effects can lead to more complex modifications via the equations of stellar structure (Thorne 1977), it is expected that differential comparisons between models will not be changed appreciably for calculations in which general relativistic effects are included and ones in which they are not.

The results of our numerical calculations produce burst properties which exhibit a wide range of diversity so characteristic of observed X-ray burst sources. Thermal and compositional inertia effects are, therefore, essential ingredients in the thermonuclear flash model, and such effects should be included when detailed comparisons between observations and theory are attempted. Future investigations are planned to determine whether the enigmatic bursts with short recurrence time scales of $\sim$5–20 minutes (e.g, MXB 1743−28, Lewin et al. 1976; EXO 0748−676, Gottwald et al. 1986; XB 1745−24, Oda 1982) characterized by α-values $\lesssim 10$ (and in some cases as low as 2) can be interpreted within this same framework.

We wish to thank the referee, J. van Paradijs, for his comments which have improved the clarity of the manuscript. This research has been supported in part by NASA under grants NAGW-830, NAGW-1284, NAGW-2525, and NAGW-2526, by NSF under grant AST 9115367, and at LLNL by the Department of Energy under grant W-7405-ENG-48.

REFERENCES

Ayasli, S., & Joss, P. C. 1982, ApJ, 256, 637
Bildsten, L., Salpeter, E. E., & Wasserman, I. 1992, ApJ, 384, 183
Fujimoto, M. Y. 1988, ApJ, 324, 995
Fujimoto, M. Y., Hanawa, T., Iben, I. Jr., & Richardson, M. B. 1984, in High Energy Transients in Astrophysics, ed. S. E. Woosley (New York: AIP), 302
———. 1987a, ApJ, 315, 198
Fujimoto, M. Y., Hanawa, T., & Miyaji, S. 1981, ApJ, 247, 267
Fujimoto, M. Y., Sztanjo, M., Lewin, W. H. G., & van Paradijs, J. 1987b, ApJ, 319, 902
Fushiki, I., & Lamb, D. Q. 1987, ApJ, 323, L55
Fushiki, I., Taam, R. E., Woosley, S. E., & Lamb, D. Q. 1992, ApJ, 390, 634
Gottwald, M., Haberl, F., Parmar, A., & White, N. E. 1986, ApJ, 308, 213
Joss, P. C. 1977, Nature, 270, 310
Lamb, D. Q., & Lamb, F. K. 1978, ApJ, 220, 291
Lambert, D. 1987, J. Astrophys. Astron., 8, 103
Lapidus, I. I., & Sunyaev, R. A. 1985, MNRAS, 217, 219
Lewin, W. H. G., Li, F. K., Hoffman, J. A., Doty, J., Buff, J., Clark, G. W., & Rappaport, S. 1976, MNRAS, 177, 93P
Lewin, W. H. G., van Paradijs, J., Cominsky, L., & Holzner, S. 1980, MNRAS, 193, 15
Lewin, W. H. G., van Paradijs, J., & Taam, R. E. 1993, Space Sci. Rev., in press
Li, F. K., Lewin, W. H. G., Clark, G. W., Doty, J., Hoffman, J. A., & Rappaport, S. A. 1977, MNRAS, 179, 21P
Melia, F., Zylstra, G. J., & Fryxell, B. 1992, ApJ, 396, L27
Murakami, T., et al. 1980, ApJ, 240, L143
Oda, M. 1982, in Gamma Ray Transients and Related Astrophysical Phenomena, ed. R. E. Lingenfelter, H. S. Hudson, & D. M. Worrall (New York: AIP), 319
Smith, G. 1987, PASP, 99, 67
———. 1988, in The Abundance Spread Within Globular Clusters, ed. G. C. de Strobel, M. Spite, & T. L. Evans (Paris: Observatoire de Paris), 63
Suntzeff, N. 1988, in The Abundance Spread Within Globular Clusters, ed. G. C. de Strobel, M. Spite, & T. L. Evans (Paris: Observatoire de Paris), 40
Taam, R. E. 1980, ApJ, 241, 351
———. 1985, Ann. Rev. Nucl. Part. Sci., 35, 1
Thorne, K. S. 1977, ApJ, 212, 825
van Paradijs, J., Penninx, W., & Lewin, W. H. G. 1988, MNRAS, 233, 437
Wallace, R. K., & Woosley, S. E. 1981, ApJS, 43, 389
Wallace, R. K., Woosley, S. E., & Weaver, T. A. 1982, ApJ, 258, 696
Weaver, T. A., Zimmerman, G. B., & Woosley, S. E. 1978, ApJ, 225, 1021
Wheeler, J., Sneden, C., & Truran, J. 1989, ARA&A, 27, 279
Woosley, S. E., & Taam, R. E. 1976, Nature, 263, 101
Woosley, S. E., & Weaver, T. A. 1985, in High Energy Transients in Astrophysics, ed. S. E. Woosley (New York: AIP), 273